



# Long-lived $K$ isomer and enhanced $\gamma$ vibration in the neutron-rich nucleus $^{172}\text{Dy}$ : Collectivity beyond double midshell



H. Watanabe<sup>a,b,c,\*</sup>, G.X. Zhang<sup>a,b</sup>, K. Yoshida<sup>d,e</sup>, P.M. Walker<sup>f</sup>, J.J. Liu<sup>g</sup>, J. Wu<sup>c,h</sup>, P.H. Regan<sup>f,i</sup>, P.-A. Söderström<sup>c</sup>, H. Kanaoka<sup>j</sup>, Z. Korkulu<sup>k</sup>, P.S. Lee<sup>l</sup>, S. Nishimura<sup>c</sup>, A. Yagi<sup>j</sup>, D.S. Ahn<sup>c</sup>, T. Alharbi<sup>m</sup>, H. Baba<sup>c</sup>, F. Browne<sup>n</sup>, A.M. Bruce<sup>n</sup>, R.J. Carroll<sup>f</sup>, K.Y. Chae<sup>o</sup>, Zs. Dombradi<sup>k</sup>, P. Doornenbal<sup>c</sup>, A. Estrade<sup>p</sup>, N. Fukuda<sup>c</sup>, C. Griffin<sup>p</sup>, E. Ideguchi<sup>q</sup>, N. Inabe<sup>c</sup>, T. Isobe<sup>c</sup>, S. Kanaya<sup>j</sup>, I. Kojouharov<sup>r</sup>, F.G. Kondev<sup>s</sup>, T. Kubo<sup>c</sup>, S. Kubono<sup>c</sup>, N. Kurz<sup>r</sup>, I. Kuti<sup>k</sup>, S. Lalkovski<sup>f</sup>, G.J. Lane<sup>t</sup>, C.S. Lee<sup>l</sup>, E.J. Lee<sup>o</sup>, G. Lorusso<sup>c,f,i</sup>, G. Lotay<sup>f</sup>, C.-B. Moon<sup>u</sup>, I. Nishizuka<sup>v</sup>, C.R. Nita<sup>n,w</sup>, A. Odahara<sup>j</sup>, Z. Patel<sup>f</sup>, V.H. Phong<sup>c,x</sup>, Zs. Podolyák<sup>f</sup>, O.J. Roberts<sup>y</sup>, H. Sakurai<sup>c</sup>, H. Schaffner<sup>r</sup>, C.M. Shand<sup>f</sup>, Y. Shimizu<sup>c</sup>, T. Sumikama<sup>v</sup>, H. Suzuki<sup>c</sup>, H. Takeda<sup>c</sup>, S. Terashima<sup>a,b</sup>, Zs. Vajta<sup>k</sup>, J.J. Valiente-Dóbon<sup>z</sup>, Z.Y. Xu<sup>g</sup>

<sup>a</sup> School of Physics and Nuclear Energy Engineering, Beihang University, Beijing 100191, China

<sup>b</sup> International Research Center for Nuclei and Particles in the Cosmos, Beihang University, Beijing 100191, China

<sup>c</sup> RIKEN Nishina Center, 2-1 Hirosawa, Wako, Saitama 351-0198, Japan

<sup>d</sup> Graduate School of Science and Technology, Niigata University, Niigata 950-2181, Japan

<sup>e</sup> Center for Computational Sciences, University of Tsukuba, Tsukuba 305-8577, Japan

<sup>f</sup> Department of Physics, University of Surrey, Guildford GU2 7XH, United Kingdom

<sup>g</sup> Department of Physics, the University of Hong Kong, Pokfulam Road, Hong Kong

<sup>h</sup> Department of Physics, Peking University, Beijing 100871, China

<sup>i</sup> National Physical Laboratory, Teddington, Middlesex, TW11 0LW, United Kingdom

<sup>j</sup> Department of Physics, Osaka University, Machikaneyama-machi 1-1, Osaka 560-0043 Toyonaka, Japan

<sup>k</sup> MTA Atomki, P.O. Box 51, Debrecen, H-4001, Hungary

<sup>l</sup> Department of Physics, Chung-Ang University, Seoul 156-756, Republic of Korea

<sup>m</sup> Department of Physics, College of Science in Zulfi, Almajmaah University, P.O. Box 1712, 11932, Saudi Arabia

<sup>n</sup> School of Computing Engineering and Mathematics, University of Brighton, Brighton, BN2 4GJ, United Kingdom

<sup>o</sup> Department of Physics, Sungkyunkwan University, Suwon 440-746, Republic of Korea

<sup>p</sup> School of Physics and Astronomy, University of Edinburgh, Edinburgh EH9 3JZ, United Kingdom

<sup>q</sup> Research Center for Nuclear Physics (RCNP), Osaka University, Ibaraki, Osaka 567-0047, Japan

<sup>r</sup> GSI Helmholtzzentrum für Schwerionenforschung GmbH, 64291 Darmstadt, Germany

<sup>s</sup> Nuclear Engineering Division, Argonne National Laboratory, Argonne, IL 60439, USA

<sup>t</sup> Department of Nuclear Physics, R.S.P.E., Australian National University, Canberra, A.C.T 0200, Australia

<sup>u</sup> Department of Display Engineering, Hoseo University, Chung-Nam 336-795, Republic of Korea

<sup>v</sup> Department of Physics, Tohoku University, Aoba, Sendai, Miyagi 980-8578, Japan

<sup>w</sup> Horia Hulubei National Institute for R&D in Physics and Nuclear Engineering (IFIN-HH), Bucharest, RO-077125, Romania

<sup>x</sup> VNU Hanoi University of Science, 334 Nguyen Trai, Thanh Xuan, Hanoi, Viet Nam

<sup>y</sup> School of Physics, University College Dublin, Belfield, Dublin 4, Ireland

<sup>z</sup> Istituto Nazionale di Fisica Nucleare, Laboratori Nazionali di Legnaro, 35020 Legnaro, Italy

## ARTICLE INFO

### Article history:

Received 22 May 2016

Accepted 21 July 2016

Available online 25 July 2016

Editor: V. Metag

## ABSTRACT

The level structure of  $^{172}\text{Dy}$  has been investigated for the first time by means of decay spectroscopy following in-flight fission of a  $^{238}\text{U}$  beam. A long-lived isomeric state with  $T_{1/2} = 0.71(5)$  s and  $K^\pi = 8^-$  has been identified at 1278 keV, which decays to the ground-state and  $\gamma$ -vibrational bands through hindered electromagnetic transitions, as well as to the daughter nucleus  $^{172}\text{Ho}$  via allowed

\* Corresponding author at: School of Physics and Nuclear Energy Engineering, Beihang University, Beijing 100191, China.

E-mail address: [hiroshi@ribf.riken.jp](mailto:hiroshi@ribf.riken.jp) (H. Watanabe).

**Keywords:**

$^{172}\text{Dy}$   
 K isomer  
 Decay spectroscopy  
 Axial symmetry  
 $\gamma$  vibration

$\beta$  decays. The robust nature of the  $K^\pi = 8^-$  isomer and the ground-state rotational band reveals an axially-symmetric structure for this nucleus. Meanwhile, the  $\gamma$ -vibrational levels have been identified at unusually low excitation energy compared to the neighboring well-deformed nuclei, indicating the significance of the microscopic effect on the non-axial collectivity in this doubly mid-shell region. The underlying mechanism of enhanced  $\gamma$  vibration is discussed in comparison with the deformed Quasiparticle Random-Phase Approximation based on a Skyrme energy-density functional.

© 2016 The Author(s). Published by Elsevier B.V. This is an open access article under the CC BY license (<http://creativecommons.org/licenses/by/4.0/>). Funded by SCOAP<sup>3</sup>.

The shape is one of the fundamental features inherent to self-confined nuclear matter consisting of a finite number of nucleons,  $Z$  protons and  $N$  neutrons. It is well known that the spherical equilibrium shape is energetically favored for closed-shell configurations. However, the sphericity tends to be unstable with the addition (or removal) of valence nucleons. When moving further away from shell closures, the nucleus is driven towards a non-spherical equilibrium shape due to the strong coupling between the motion of the individual valence nucleons and the surface oscillations of the closed-shell core [1–3]. Such a phenomenon of spontaneous symmetry breaking is analogous to the so-called “Jahn–Teller effect” in polyatomic molecules [4].

The excitation spectrum in deformed nuclei is characterized by rotational and vibrational motion, the latter corresponding to oscillations around the equilibrium shape with a fixed orientation of the nucleus. For axially symmetric nuclei, the lowest order shape vibration is of quadrupole type (i.e., a phonon carries two units of angular momentum), which can be classified into two modes,  $\beta$  and  $\gamma$  vibrations [5], in terms of the component of (vibrational) angular momentum along the symmetry axis, denoted by  $K$ . The  $\beta$ -vibrational mode with  $K^\pi = 0^+$  maintains axial symmetry, while the  $K^\pi = 2^+$   $\gamma$  vibration represents a dynamical distortion from axial symmetry, which may prelude the emergence of  $\gamma$  instability or rigid triaxial deformation approaching the transitional region where the nuclei have less-deformed quadrupole shapes.

In the present work, we have explored neutron-rich Dy isotopes ( $Z = 66$ ) with a particular focus on the systematic behavior of the ground-state (g.s.) and  $\gamma$ -vibrational bands. Based on a simple assumption that the axial quadrupole deformation increases as the number of valence nucleons increases, it is conjectured that the maximum ground-state deformation occurs in the doubly mid-shell nucleus  $^{170}\text{Dy}$  ( $N = 104$ ). In actual nuclei, however, the stability of shape is likely to be sensitive to characteristic single-particle (Nilsson) orbitals near the Fermi surface. For instance, the low-frequency  $\gamma$ -vibrational mode can be induced by two-quasiparticle (2qp) excitations involving Nilsson orbits  $K^\pi [Nn_z\Lambda]$  that satisfy the selection rules,  $\Delta N = \Delta n_z = 0$ ,  $\Delta \Lambda = \pm 2$ , and  $\Delta K = \pm 2$  [6]. Experimentally, the existence of  $\gamma$ -vibrational levels at low excitation energy can be a signature of softening deformed shape with respect to the axially-asymmetric ( $\gamma$ ) degree of freedom. In this Letter, we will report on the first spectroscopic results of the g.s. and  $\gamma$  bands in  $^{172}\text{Dy}$  ( $N = 106$ ), the most neutron-rich Dy isotope studied to date. Its excited states have been populated through the decay from a long-lived metastable state (isomer [7]), which has the same configuration as the  $K^\pi = 8^-$  isomers that had been identified in the  $N = 106$  isotones from  $Z = 68$  to 82 [8]. Thus, the present work has extended a sequence of the  $N = 106$  isomers to the previously inaccessible nucleus of  $Z = 66$ . It is notable that high- $K$  isomers can serve as a useful probe for the underlying nuclear structure since their nature is sensitive to intrinsic orbits near the Fermi surface, pairing and other residual interactions, and the degree of axial symmetry [9].

Concerning astrophysical interest, it has been suggested that the nuclear deformation of neutron-rich rare-earth isotopes plays

an important role in the formation of a pygmy peak around  $A = 160$  in the  $r$ -process solar abundance distribution [10]. Despite such a broad range of interest, spectroscopic information still remains scarce due to the experimental difficulties in producing neutron-rich nuclei around and beyond the double midshell. The advent of the third-generation in-flight fragment separator facility, the RI-Beam Factory (RIBF) at RIKEN [11], enables access to this exotic area and allows for systematic studies of their decay properties. So far,  $^{172}\text{Dy}$  is the heaviest isotope for which any new information on the excited-level structure has been obtained at RIBF. Hence, this Letter provides significant insight into the nuclear shape and collectivity in this hard-to-reach region of well-deformed nuclei.

Neutron-rich nuclei around  $A = 170$  were produced by in-flight fission of a  $^{238}\text{U}^{86+}$  beam at 345 MeV/u with an average intensity of 12 pnA. The nuclei of interest were separated and identified through the BigRIPS separator [12]. Identification of particles with the atomic number ( $Z$ ) and the mass-to-charge ratio ( $A/q$ ) was achieved on the basis of the  $\Delta E$ -TOF- $B\rho$  method, in which the energy loss ( $\Delta E$ ), time of flight (TOF), and magnetic rigidity ( $B\rho$ ) were measured using the focal-plane detectors on the beam line. The secondary beams were transported with two different settings of the slits on the beam line; one is optimized for  $^{170}\text{Dy}^{66+}$ , and the other for  $^{172}\text{Dy}^{66+}$ . The obtained particle-identification spectra are shown in Ref. [13]. The resolution of the mass-to-charge ratio ( $\lesssim 0.05\%$ ) was sufficient to separate nearby hydrogen-like ions. The identified particles were implanted into WAS3ABi [14], which consisted of two double-sided silicon-strip detectors (DSSSD) stacked compactly. Each DSSSD had a thickness of 1 mm with an active area segmented into sixty and forty strips (1-mm pitch) on each side in the horizontal and vertical dimensions, respectively. The DSSSDs also served as detectors for electrons following  $\beta$ -decay and internal conversion (IC) processes [15]. Gamma rays were detected by the EURICA spectrometer [14]. The  $\gamma$ -ray measurements were carried out within a time range up to 100  $\mu\text{s}$  relative to the trigger signal generated either from a plastic scintillation counter placed at the end of the beam line or from WAS3ABi. About  $7.1 \times 10^3$   $^{172}\text{Dy}$  ions were implanted into WAS3ABi during the experiment.

Prior to the present work, no spectroscopic information had been reported for  $^{172}\text{Dy}$ . Fig. 1(a) exhibits a  $\gamma$ -ray energy spectrum measured within 4 s after the implantation of  $^{172}\text{Dy}$  with a gate on an electron energy ranging from 0 to 230 keV. Since such low-energy signals arise predominantly from IC electrons rather than from  $\beta$  particles, the  $\gamma$  transitions observed under this gate condition can be associated with the decay from a long-lived isomer in the implanted nucleus. The measured X-ray energy at 45.8 keV is in good agreement with the  $K_\alpha$  lines for Dy atoms.

The level scheme of  $^{172}\text{Dy}$  established in the present work is displayed in Fig. 2. In the  $A \sim 170$  region of interest, the level sequence of the g.s. rotational band in even–even nuclei is similar to that of the neighboring isotopes and unlikely to change drastically with the proton or neutron number. Therefore, based on the systematics for lighter Dy isotopes and heavier  $N = 106$  isotones [16], the transitions of 76, 175, 269, and 358 keV are

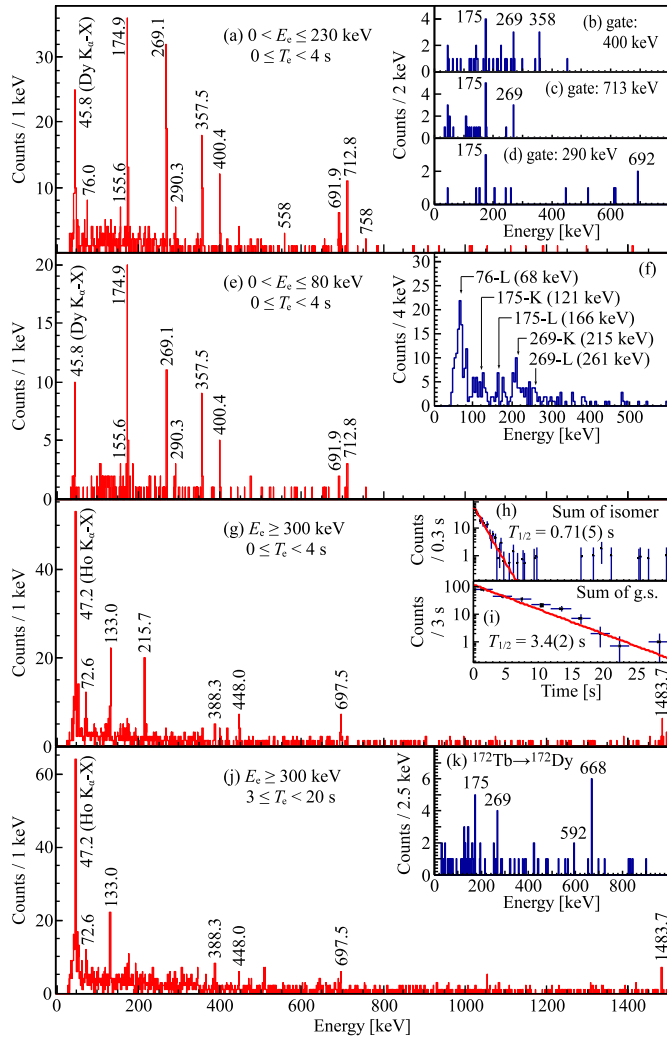


**Fig. 1.** (Color online) (a)(e)(g)(j):  $\gamma$ -ray energy spectra measured with gates on electron energy ( $E_e$ ) and time ( $T_e$ ) as indicated after implantation of  $^{172}\text{Dy}$  ions. (b)(c)(d):  $\gamma$  rays in coincidence with specific transitions as indicated. (f): Electron energy spectrum measured with a sum of gates on isomeric-decay transitions. The arrows point to the energies of the respective  $K$ - and  $L$ -conversion electrons. (h)(i): Time distributions and associated fits for  $\gamma$  rays following the isomer and ground-state (g.s.) decays. (k):  $\gamma$  rays measured within 0–1.3 s following the  $^{172}\text{Tb}$  implantation.

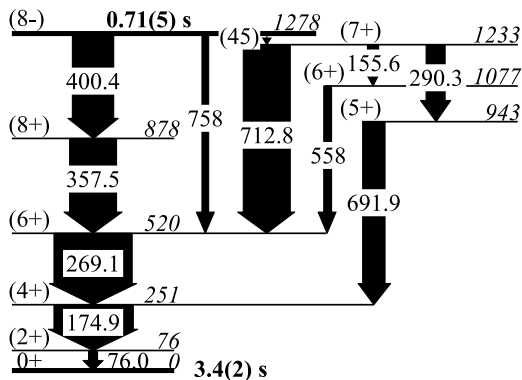


**Fig. 2.** Partial level scheme of  $^{172}\text{Dy}$  constructed in the present work. The widths of arrows are proportional to the  $\gamma$ -ray intensities summarized in Table 1, except for the 45- and 76-keV transitions.

**Table 1**  
Summary of transitions from the  $K^\pi = 8^-$  isomer in  $^{172}\text{Dy}$ .

$E_\gamma$ [keV]	$I_\gamma$ [rel.] <sup>a</sup>	$I_{\text{tot}}^b$	$\alpha_f^{\text{cal}}$ [17]	$\sigma\lambda$	$J_i^\pi \rightarrow J_f^\pi$
45	...	...	0.472	E1	$(8_1^-) \rightarrow (7_1^+)$
76.0(4)	...	...	7.67	E2	$(2_1^+) \rightarrow 0_1^+$
155.6(8)	17(8)	29(14)	0.682	M1	$(7_1^+) \rightarrow (6_2^+)$
174.9(1)	215(62)	294(86)	0.371	E2	$(4_1^+) \rightarrow (2_1^+)$
269.1(1)	179(52)	196(57)	0.090	E2	$(6_1^+) \rightarrow (4_1^+)$
290.3(4)	40(13)	43(14)	0.072	E2	$(7_1^+) \rightarrow (5_1^+)$
357.5(1)	125(43)	130(45)	0.038	E2	$(8_1^+) \rightarrow (6_1^+)$
400.4(2)	100(35)	101(36)	0.008	E1	$(8_1^-) \rightarrow (8_1^+)$
558(1)	19(10)	19(10)	0.011	E2	$(6_2^+) \rightarrow (6_1^+)$
691.9(4)	56(17)	57(17)	0.007	E2	$(5_1^+) \rightarrow (4_1^+)$
712.8(2)	99(35)	100(35)	0.006	E2	$(7_1^+) \rightarrow (6_1^+)$
758(1)	15(8)	15(8)	0.028	M2	$(8_1^-) \rightarrow (6_1^+)$

<sup>a</sup> Relative to the  $\gamma$ -ray intensity of the 400-keV transition.

<sup>b</sup>  $I_{\text{tot}} = (1 + \alpha_f^{\text{cal}})I_\gamma$ .

assigned as  $2_1^+ \rightarrow 0_1^+$ ,  $4_1^+ \rightarrow 2_1^+$ ,  $6_1^+ \rightarrow 4_1^+$ , and  $8_1^+ \rightarrow 6_1^+$ , respectively. The latter three transitions are found to be in mutual coincidence, as well as with a  $\gamma$  ray at 400 keV [see Figs. 1(b)]. Based on this, we propose a state at 1278 keV as a  $K^\pi = 8^-$  isomer, which feeds the  $8_1^+$  level via a hindered E1 transition, consistent with what was observed for the heavier  $N = 106$  isotones [8].

In addition to the 400–358–269–175–76-keV cascade, several other  $\gamma$  rays are visible in Fig. 1(a). The 758-keV transition is assigned as a weak M2 branch from the  $8^-$  isomer to the  $6_1^+$  state on account of the consistency in energy with the sum of 400 and 358 keV. Gamma-gamma coincidence analyses reveal that the  $\gamma$  ray at 713 keV is in coincidence with the 175- and 269-keV transitions, but neither with the 358- nor 400-keV transitions [Fig. 1(c)], while the 290- and 692-keV  $\gamma$  rays are in mutual coincidence and with the 175-keV line [Fig. 1(d)]. The energy matching for these cascades suggests the presence of a 45-keV transition from the 1278-keV isomer to an intermediate state at 1233 keV, though the corresponding  $\gamma$  line could not be separated from the intense Dy  $K_\alpha$ -X ray. The placement of the 1233-keV state below the  $8^-$  isomer is additionally supported by the observation of  $\gamma$  rays at 156 and 558 keV, the sum of their energies in agreement with 713 keV within errors. The orders of the 290–692- and 156–558-keV transitions could not be determined from the present analysis of  $\gamma$ - $\gamma$  coincidence and  $\gamma$ -ray intensity. However, the proposed sequence of the non-yrast levels in Fig. 2 will be justified later based on the arguments of the moment of inertia and the decay pattern towards the g.s. rotational band. A half-life of 0.71(5) s has been derived from a least-squares fit of the summed  $\gamma$ -ray gated time spectra for the isomeric-decay transitions, as shown in Fig. 1(h).

It should be noted that in Fig. 1(a) the intensity of the 76-keV  $\gamma$  ray is much weaker than that of the preceding transitions of 175 and 269 keV, because this low-energy E2 transition is highly converted. The 76-keV  $\gamma$  transition becomes visible when it is not converted, and when the IC electrons for the other transitions in cascade are detected. As demonstrated in Fig. 1(e), the 76-keV  $\gamma$  ray disappears with a gate on an electron energy only up to 80 keV, where the  $L$ -conversion electrons for the 76-keV transition are predominant [see a  $\gamma$ -ray gated electron energy spectrum in Fig. 1(f)]. Note that the energy of the  $K$ -conversion electrons for the 76-keV transition is below the threshold of the DSSSDs. The relative  $\gamma$ -ray intensities ( $I_\gamma$ ) evaluated with this electron gating condition are summarized in Table 1. For all the intermediate levels, excepting the 76- and 1233-keV states, the total transition intensities ( $I_{\text{tot}}$ ), including IC, are well balanced between the incoming and outgoing transitions.

Spins of 5, 6, and 7 are tentatively assigned for the states at 943, 1077, and 1233 keV, respectively, based on the observed feeding patterns towards the members of the g.s. rotational band. Con-

cerning the parity of these levels, if they had negative parity, the  $K^\pi = 8^-$  isomer would preferentially decay towards the 1077-keV state via an  $E2$  transition. Because such a  $\gamma$  ray has not been observed in this experiment, we propose positive parity to these levels. Essentially, in all deformed even–even nuclei, the non-yrast level sequence with positive parity, including odd-spin states, below the pairing-gap energy,  $2\Delta \sim 1.5$  MeV, is the best candidate for a  $K^\pi = 2^+$   $\gamma$ -vibrational band. With this as an assumption, the moment of inertia for the 290-keV,  $(7_1^+) \rightarrow (5_1^+)$  transition is estimated to be  $44.8 \hbar^2 \text{MeV}^{-1}$ . This is somewhat larger than that of the g.s. band at low rotational frequencies, 39.5 ( $2_1^+ \rightarrow 0_1^+$ ), 40.0 ( $4_1^+ \rightarrow 2_1^+$ ), 40.9 ( $6_1^+ \rightarrow 4_1^+$ ),  $42.0 \hbar^2 \text{MeV}^{-1}$  ( $8_1^+ \rightarrow 6_1^+$ ), as is also found for the neighboring even–even nuclei, supporting the assignment of the  $\gamma$ -band levels.

The proposed  $\gamma$ -band levels are found to preferentially decay towards the g.s. rotational band rather than its lower-spin members; the energies of unpopulated states are estimated to be 671 ( $2_2^+$ ), 739 ( $3_2^+$ ), and 830 keV ( $4_2^+$ ) from an extrapolation of the observed  $\gamma$ -band levels based on the standard rotational-energy equation. This result can be explained by  $\Delta K = 2$  mixing between the g.s. and  $\gamma$ -vibrational bands, as outlined in Ref. [18]. First, we consider the decay branches from the  $7_2^+$  state at 1233 keV. With the spin independent mixing amplitude  $\epsilon$  of the  $\gamma$ -band state into the g.s.-band state (or vice versa), the  $E2$  reduced transition probability for the  $7_2^+ \rightarrow 6_2^+$  inter-band transition can be written as

$$B(E2; 7_2^+ \rightarrow 6_2^+) = B'(E2; 7_2^+ \rightarrow 6_2^+) \left[ 1 - \epsilon f_6 \frac{\sqrt{B'(E2; 7_2^+ \rightarrow 6_2^+)}}{\sqrt{B'(E2; 7_2^+ \rightarrow 6_2^+)}} \right]^2$$

where  $f_6 = \sqrt{2 \cdot 5 \cdot 6 \cdot 7 \cdot 8}$  represents the spin dependent part of the  $\Delta K = 2$  mixing amplitude between the (unperturbed)  $6_2^+$  and  $6_2^+$  states.  $B'(E2)$  denotes the unperturbed value defined as follows,

$$B'(E2; 7_2^+ \rightarrow 6_2^+) = 2(722 - 2|60\rangle^2 \langle \text{g.s.} | E2 | \gamma \rangle^2,$$

$$B'(E2; 7_2^+ \rightarrow 6_2^+) = \frac{5}{16\pi} e^2 Q_0^2 \langle 7220 | 62 \rangle^2,$$

where  $\langle J_i K_i 2 \Delta K | J_f K_f \rangle$  is the Clebsch–Gordan coefficient,  $Q_0$  and  $\langle \text{g.s.} | E2 | \gamma \rangle$  represent the intrinsic quadrupole moment and the unperturbed  $E2$  matrix element between the g.s. and  $\gamma$  bands, respectively. On the other hand, the  $7_2^+ \rightarrow 5_2^+$  in-band transition is immune from the g.s.- $\gamma$  mixing (because they have odd spins), that is,

$$B(E2; 7_2^+ \rightarrow 5_2^+) = B'(E2; 7_2^+ \rightarrow 5_2^+) = \frac{5}{16\pi} e^2 Q_0^2 \langle 7220 | 52 \rangle^2.$$

The mixing amplitude can be determined to be  $\epsilon = 1.5 \times 10^{-3}$  from the  $B(E2)$  ratio

$$R(7_2^+) = \frac{B(E2; 7_2^+ \rightarrow 6_2^+)}{B(E2; 7_2^+ \rightarrow 5_2^+)} = \frac{I_\gamma(7_1^+ \rightarrow 6_1^+)}{I_\gamma(7_1^+ \rightarrow 5_1^+)} \times \left( \frac{290.3}{712.8} \right)^5,$$

using the relative  $\gamma$ -ray intensities in Table 1 and  $Q_0 = 7.5$  eb,  $\langle \text{g.s.} | E2 | \gamma \rangle = 0.35$  eb estimated for  $^{172}\text{Dy}$  [19]. With this in hand, the  $B(E2)$  ratio for the decays from the  $5_2^+$  state at 943 keV can be estimated in a similar way to be  $R(5_2^+) = 5.2 \times 10^{-2}$ . Providing the extrapolated energy of 739 keV for the unobserved  $3_2^+$  state, a competing  $5_2^+ \rightarrow 3_2^+$  in-band transition (204 keV) is expected to have a  $\gamma$ -ray intensity of 4.3% relative to the  $5_2^+ \rightarrow 4_2^+$  inter-band

**Table 2**

Transition strengths and hindrances for decays from the  $K^\pi = 8^-$  isomer in  $^{172}\text{Dy}$ .

Transition	$I_{\text{tot}}$ (%)	$\sigma\lambda$	$B(\sigma\lambda)$ (W.u.)	$\nu$	$f_\nu$
45 keV $\gamma$	48(15)	E1	$1.1(3) \times 10^{-12}$	5	247(15)
400 keV $\gamma$	28(12)	E1	$1.4(6) \times 10^{-15}$	7	133(8)
758 keV $\gamma$	4(2)	M2	$2.4(13) \times 10^{-10}$	6	40(4)
$\beta$ decay	19(3)	...	...	...	...

transition. It would be hard to explicitly observe this small fraction due to the statistics obtained in the present work.

The low-lying states of  $^{172}\text{Dy}$  have also been investigated by the  $\beta$  decay from  $^{172}\text{Tb}_{107}$ . As shown in Fig. 1(k), the 175- and 269-keV  $\gamma$  rays are observed clearly in this decay channel, indicating the presence of a  $\beta$ -decaying state with  $J^\pi = 5^+$ ,  $6^+$ , or  $7^+$  in the parent nucleus. The Nilsson levels,  $\pi 3/2^+[411]$  and  $\nu 9/2^+[624]$ , are assigned to the ground states of well-deformed odd- $A$  Tb isotopes and  $N = 107$  isotones, respectively [16]. Thus, based on the rule of Gallagher and Moszkowski [20], the ground state of  $^{172}\text{Tb}$  is expected to have  $J^\pi = 6^+$  with the  $\pi 3/2^+[411] \otimes \nu 9/2^+[624]$  configuration. Meanwhile, the anti-parallel coupling of the intrinsic spins with this configuration would yield a  $3^+$  state at low excitation energy, leading to the possibility of a long lifetime owing to the large spin gap with respect to the ground state. Such a long-lived isomer could be also populated via fission of  $^{238}\text{U}$  and undergo  $\beta$  decay towards low-spin states ( $J \sim 2$ ) in the daughter nucleus. Fig. 1(k) shows other  $\gamma$ -ray peaks at 668 and 592 keV, in agreement with the extrapolated energy of the  $2_2^+$  state (671 keV) and its energy difference with respect to the  $2_1^+$  level, respectively. Although these are possible candidates for the transitions de-exciting the  $2_2^+$  state, more statistics will be required to confirm its decay scheme. In the following discussion on the  $\gamma$ -vibrational levels, therefore, we will adopt an extrapolated energy of 671 keV for the  $2_2^+$  state.

Besides the internal decay branches, the  $T_{1/2} = 0.71$  s isomer decays externally towards the daughter nucleus  $^{172}\text{Ho}_{105}$ . Figs. 1(g) and 1(j) show  $\gamma$ -ray energy spectra measured by gating on an electron energy of 300 keV and higher, where  $\beta$  rays are predominant over IC electrons, as is evident from the observation of the Ho  $K_\alpha$ -X ray at 47.2 keV. For this analysis, two different time windows are applied to increase the sensitivity to  $\gamma$  rays following the  $\beta$  decays from shorter- and longer-living states. The 216-keV  $\gamma$  ray disappears for the longer time range in Fig. 1(j), while other peaks at 73, 133, 388, 448, 698, and 1484 keV can be observed for both the time windows. The latter  $\gamma$  rays are believed to arise from the  $\beta$  decay of the  $^{172}\text{Dy}$  ground state, which has a longer half-life [ $T_{1/2} = 3.4(2)$  s, see Fig. 1(i)] than the isomer. Meanwhile, the 216-keV transition, which exhibits a similar time behavior to the internal decay branches, is expected to follow the  $\beta$  decay from the  $K^\pi = 8^-$  isomer. The  $\beta$ -decay branching ratio from the  $^{172}\text{Dy}$  isomer is estimated to be 19(3)% with the assumption that all the  $\beta$ -decay intensity flows into the 216-keV transition. In this analysis, the efficiency ratio of the IC electrons to the  $\beta$  rays is taken into account [21]. The measured  $\beta$ -branching ratio yields  $\log ft = 5.0(2)$  using  $T_{1/2} = 0.71(5)$  s and  $Q_\beta = 3470(360)$  keV [22]. Note that this  $\log ft$  value is obtained for a possible  $\beta$  feeding directly towards an excited state at 216 keV in  $^{172}\text{Ho}$ ; in case the state to which the 216-keV transition decays is *not* the ground state, the  $\log ft$  value becomes smaller as its excitation energy increases. The observation of the small  $\log ft$  value indicates the occurrence of an allowed  $\beta$  transition from the  $K^\pi = 8^-$  isomer of  $^{172}\text{Dy}$ . The branching ratios for both the internal and external decays are summarized in Table 2.

In the  $N = 106$  isotones, the energies of the  $K^\pi = 8^-$  isomers, which are interpreted as arising from the same neutron 2qp



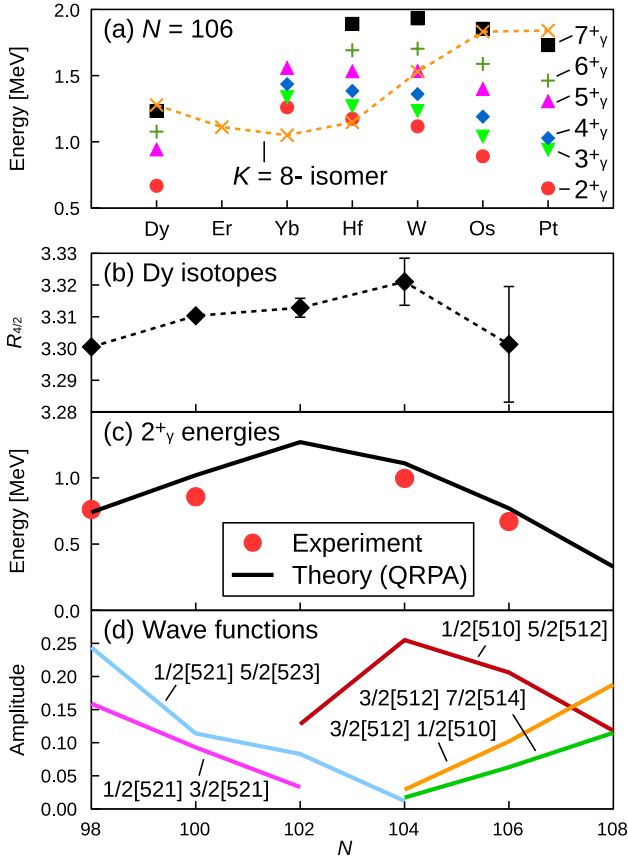


**Fig. 3.** (Color online) (a): Energy systematics of the  $\gamma$ -vibrational bands and  $K^\pi = 8^-$  isomers, connected by the dashed line, for  $N = 106$  isotones. (b): Energy ratios  $R_{4/2} = E(4_1^+)/E(2_1^+)$  of the g.s. rotational bands in even–even Dy isotopes. (c): Energies of the  $K^\pi = 2^+$   $\gamma$ -vibrational band heads. The results of QRPA calculations using the SkM\* functional are also depicted. (d): Amplitudes squared of the neutron 2qp components in the QRPA wave functions for the  $\gamma$ -vibrational mode. The experimental data are taken from Refs. [16,8,23] and the present work. The  $2_1^+$  energy of  $^{172}\text{Dy}$  is extrapolated from the observed  $\gamma$ -vibrational levels.

configuration,  $\nu 7/2^- [514] \otimes \nu 9/2^+ [624]$  [24], decrease when the proton number decreases to  $Z = 70$  (Yb) and subsequently rise towards  $^{172}\text{Dy}$ , as shown in Fig. 3(a). The energy systematics from  $^{184}\text{Pt}$  to  $^{174}\text{Er}$  can be understood in terms of the variation of the neutron pairing strength [8]. The isomerism is essentially ascribed to the large difference in the  $K$  quantum number between the isomer and the states to which the isomer decays. For the  $E1$  transition from the  $K^\pi = 8^-$  isomer to the  $8_1^+$  state in the  $K^\pi = 0^+$  g.s. band, which has forbiddenness  $\nu = \Delta K - \lambda = 7$  ( $\lambda$  is the multipolarity), the so-called reduced hindrances,  $f_\nu = (T_{1/2}^\gamma/T_{1/2}^W)^{1/\nu}$ , where  $T_{1/2}^\gamma$  and  $T_{1/2}^W$  represent the partial half-life and the Weisskopf estimate, respectively, increase from 28 in  $^{188}\text{Pb}$  to 98 in  $^{174}\text{Er}$  (see Fig. 5 in Ref. [25]). The present result of  $^{172}\text{Dy}$ ,  $f_\nu = 133(8)$ , follows the upward trend in the  $N = 106$  isotones, implying that the  $K$  quantum number is rather robust, as expected for well-deformed axially symmetric nuclei.

The  $K^\pi = 8^-$  isomer in  $^{172}\text{Dy}$  is found to decay to the lower-lying  $7_1^+$  level in addition to the g.s. band. Such  $E1$ ,  $\nu = 5$  isomeric transitions were also reported for the heavier  $N = 106$  isotones,  $^{184}\text{Pt}$  and  $^{188}\text{Pb}$  [24]. For all these cases, the  $f_\nu(E1)$  value obtained for the  $\nu = 5$  branch is larger than that for the  $\nu = 7$  transition feeding the g.s. band by a factor of  $\sim 2$ . As for the  $M2$  decay from the  $K^\pi = 8^-$  isomer, the present value of  $f_\nu = 40(4)$  is comparable to a lower limit suggested for the corresponding transition in  $^{174}\text{Er}$  [25], but smaller than that of  $^{178}\text{Hf}$  [24], being partly at-

tributed to the known admixture of the proton 2qp configuration in the  $K^\pi = 8^-$  isomeric state in  $^{178}\text{Hf}$  [26,27].

It is noteworthy that in the  $N = 106$  isotonic chain the  $\gamma$ -vibrational states abruptly fall in energy in  $^{172}\text{Dy}$ , compared to the corresponding levels in  $^{176}\text{Yb}$  and  $^{178}\text{Hf}$ , as seen in Fig. 3(a). (The  $\gamma$  band has not been identified in the intervening isotone  $^{174}\text{Er}$  to date.) Indeed, the extrapolated energy of the  $2_1^+$  state in  $^{172}\text{Dy}$  is as low as that in the transitional nucleus  $^{184}\text{Pt}$ , which reveals the energy staggering in the low-spin  $\gamma$ -band levels that is characteristic of a  $\gamma$ -unstable nucleus [28]. In general, the lowering of the  $K^\pi = 2^+$   $\gamma$  band would invoke an enhancement of axial asymmetry, which most likely causes  $K$ -mixing in the final states, and therefore, results in a significant reduction of  $f_\nu$ . For example, anomalously low  $f_\nu$  values ( $\lesssim 10$ ) have been reported for typical  $\gamma$ -soft nuclei,  $^{190}\text{W}_{116}$  [29] and  $^{192}\text{Os}_{116}$  [30]. In the case of  $^{172}\text{Dy}$ , however, the  $K^\pi = 8^-$  isomer reveals the robust nature of an axially deformed nucleus, as mentioned in the previous paragraph. In this context, it is unlikely that the observed fall of the  $\gamma$ -vibrational states in  $^{172}\text{Dy}$  is ascribed to the macroscopic effect of axial asymmetry, regardless of its nature being either large amplitude  $\gamma$ -soft dynamics or static triaxiality. This conjecture is supported by inspection of the g.s. rotational band; the  $4_1^+$  state at 251 keV is sufficiently lower than the extrapolated  $2_1^+$  state at 671 keV, being at variance with the well-known feature of an axially-asymmetric rotor, in which these states are nearly degenerate. Furthermore, the energy ratio  $R_{4/2} = E(4_1^+)/E(2_1^+) = 3.30$  for  $^{172}\text{Dy}$  remains close to the limit for a symmetric rotor (3.33). Thus, all these arguments point to an axially-symmetric structure for  $^{172}\text{Dy}$ .

The  $R_{4/2}$  values for the even–even Dy isotopes saturate at  $N = 104$ , as shown in Fig. 3(b), indicative of the maximum quadrupole deformation of the ground state occurring for the doubly mid-shell nucleus  $^{170}\text{Dy}$ . This result will serve as a benchmark for testing various model calculations which predict different neutron numbers for deformation maximum [31–34].

To understand the underlying mechanism of the observed lowering of the  $\gamma$ -vibrational band, we have performed model calculations based on a Skyrme energy-density-functional (EDF). With the use of the SkM\* functional [35], the ground states are calculated by the Hartree–Fock–Bogoliubov (HFB) method, while the Quasi-particle Random-Phase Approximation (QRPA) is employed for the intrinsic excitations. The details about the theoretical model will be presented in Ref. [36]. Similar Skyrme-EDF calculations for the  $\gamma$  vibration in less neutron-rich rare-earth nuclei have been reported in Refs. [37,38], while the separable approximation was made in Ref. [38].

As demonstrated in Fig. 3(c), the HFB+QRPA calculation reproduces the experimental results very well, in particular the decreasing trend of the  $2_1^+$  energies from  $^{170}\text{Dy}$  to  $^{172}\text{Dy}$ . This can be interpreted in terms of the 2qp components involved in the QRPA wave functions, which satisfy the selection rules of the asymptotic quantum number for the non-axial quadrupole matrix element [6]. Concerning the proton configurations, the  $\pi 1/2^+ [411] \otimes \pi 3/2^+ [411]$  and  $\pi 1/2^+ [411] \otimes \pi 5/2^+ [413]$  components play an important role in generating the  $\gamma$  vibration for the Dy isotopes considered in Fig. 3(c). Since the amplitude squared of these proton components, 0.25 and 0.19 on average, respectively, does not change so much with the neutron number, the energy variation of the  $2_1^+$  states depends mainly on the neutron configuration. As exhibited in Fig. 3(d), the  $\nu 1/2^- [510] \otimes \nu 5/2^- [512]$  component dominates the neutron wave function in  $^{170}\text{Dy}$ . While the amplitude of this neutron 2qp component decreases as the neutron number increases, the other two components,  $\nu 3/2^- [512] \otimes \nu 7/2^- [514]$  and  $\nu 3/2^- [512] \otimes \nu 1/2^- [510]$ , become significant aspects of the

neutron wave function instead. In  $^{172}\text{Dy}$ , it is expected that a coherent superposition of these three neutron excitations gives rise to the enhancement of  $\gamma$  vibration, resulting in the lowered  $2^+_{\gamma}$  energy. The quadrupole transition strength to the  $\gamma$ -vibrational mode is predicted to be larger for the neutron excitation than for proton [36].

The HFB+QRPA calculation suggests that the  $2^+_{\gamma}$  state has an even lower energy in  $^{174}\text{Dy}_{108}$  [36], which was unreachable in the present experiment. The predicted energy (0.33 MeV) is lower than the  $2^+_{\gamma}$  energies of the  $N = 116$  isotones,  $^{190}\text{W}$  and  $^{192}\text{Os}$ , which are known to have the  $\gamma$ -soft nature. Of great interest will be to investigate the collectivity further beyond the neutron midshell in future experiments using more intense RI beams.

In summary, new spectroscopic results have been obtained for the neutron-rich nucleus  $^{172}\text{Dy}$ , including its previously unknown level sequences of the ground-state and  $\gamma$ -vibrational bands populated in the decay of a long-lived isomer with  $K^{\pi} = 8^-$ . It is revealed that the  $\gamma$  vibration is remarkably enhanced in this well-deformed nucleus due to simultaneous excitation of several two-quasiparticle configurations near the Fermi surface that induce the non-axial collective motion. The present work has proven the capability of the RIBF facility to produce neutron-rich rare-earth isotopes, and therefore, will pave the way to studying the evolution of nuclear shape in this hard-to-reach region.

## Acknowledgements

We are indebted to the facility crews who provided the beams at RIBF, cooperated by RIKEN Nishina Center and CNS, University of Tokyo, the EUROBALL Owners Committee for the loan of germanium detectors, the PreSpec Collaboration for the use of the readout electronics. Part of the WAS3ABi was supported by the Rare Isotope Science Project which is funded by MSIP and NRF of Korea. We thank Prof. G.D. Dracoulis for valuable suggestions. This work was supported by JSPS KAKENHI Grant No. 24740188, 25247045, and 25287065, STFC (UK authors) and the UK National Measurement Office (PHR), the U.S. Department of Energy, Office of Science, Office of Nuclear Physics under Contract No. DE-AC02-06CH11357 (FGK), NRF Korea Grants No. 2009-0093817 and 2013R1A1A2063017 (CSL), 2014S1A2A2028636 and 2016K1A3A7A09005579 (KYC), and Science Foundation Ireland under Grant No. 12/IP/1288 (OJR). The numerical calculations were performed on SR16000 at YITP, Kyoto University, and on COMA (PACS-IX) at CCS, University of Tsukuba.

## References

- [1] A. Bohr, Kgl Danske, Videnskab Selskab, Mat.-Fys. Medd. 26 (14) (1952).
- [2] D.L. Hill, J.A. Wheeler, Phys. Rev. 89 (1953) 1102.
- [3] A. Bohr, B.R. Mottelson, Kgl Danske, Videnskab Selskab, Mat.-Fys. Medd. 27 (16) (1953).
- [4] H.A. Jahn, E. Teller, Proc. R. Soc. 161 (905) (1937) 220.
- [5] K. Alder, A. Bohr, T. Huus, B. Mottelson, A. Winther, Rev. Mod. Phys. 28 (1956) 432.
- [6] B.R. Mottelson, S.G. Nilsson, Mat. Fys. Skr. Dan. Vid. Selsk. 1 (8) (1959).
- [7] G.D. Dracoulis, P.M. Walker, F.G. Kondev, Rep. Prog. Phys. 79 (2016) 076301.
- [8] G.D. Dracoulis, G.J. Lane, F.G. Kondev, A.P. Byrne, R.O. Hughes, P. Nieminen, H. Watanabe, M.P. Carpenter, R.V.F. Janssens, T. Lauritsen, D. Seweryniak, S. Zhu, P. Chowdhury, F.R. Xu, Phys. Lett. B 635 (4) (2006) 200.
- [9] G.D. Dracoulis, Phys. Scr. 2013 (T152) (2013) 014015.
- [10] R. Surman, J. Engel, J.R. Bennett, B.S. Meyer, Phys. Rev. Lett. 79 (1997) 1809.
- [11] Y. Yano, Nucl. Instrum. Methods B 261 (2007) 1009.
- [12] N. Fukuda, T. Kubo, T. Ohnishi, N. Inabe, H. Takeda, D. Kameda, H. Suzuki, Nucl. Instrum. Methods B 317 (2013) 323.
- [13] H. Watanabe, AIP Conf. Proc. 1681 (2015) 030009.
- [14] S. Nishimura, Prog. Theor. Exp. Phys. (2012) 03C006.
- [15] H. Watanabe, G. Lorusso, S. Nishimura, T. Otsuka, K. Ogawa, Z.Y. Xu, T. Sumikama, P.-A. Söderström, P. Doornenbal, Z. Li, F. Browne, G. Gey, H.S. Jung, J. Taprogge, Z. Vajta, J. Wu, A. Yagi, H. Baba, G. Benzoni, K.Y. Chae, F.C.L. Crespi, N. Fukuda, R. Gernhäuser, N. Inabe, T. Isobe, A. Jungclaus, D. Kameda, G.D. Kim, Y.K. Kim, I. Kojouharov, F.G. Kondev, T. Kubo, N. Kurz, Y.K. Kwon, G.J. Lane, C.-B. Moon, A. Montaner-Pizá, K. Moschner, F. Naqvi, M. Niikura, H. Nishibata, D. Nishimura, A. Odahara, R. Orlandi, Z. Patel, Z. Podolyák, H. Sakurai, H. Schaffner, G.S. Simpson, K. Steiger, H. Suzuki, H. Takeda, A. Wendt, K. Yoshinaga, Phys. Rev. Lett. 113 (2014) 042502.
- [16] <http://www.nndc.bnl.gov/ensdf/>.
- [17] T. Kibédi, T.W. Burrows, M.B. Trzhaskovskaya, P.M. Davidson, C.W. Nestor, Nucl. Instrum. Methods A 589 (2008) 202.
- [18] R.F. Casten, Nuclear Structure from Simple Perspective, Oxford University Press, Oxford, 2000.
- [19] K. Yoshida (private communication).
- [20] C.J. Gallagher, S.A. Moszkowski, Phys. Rev. 111 (1958) 1282.
- [21] J.J. Liu (to be submitted).
- [22] M. Wang, G. Audi, A.H. Wapstra, F.G. Kondev, M. MacCormick, X. Xu, B. Pfeiffer, Chin. Phys. C 36 (12) (2012) 1603.
- [23] P.-A. Söderström, submitted for publication.
- [24] F.G. Kondev, G.D. Dracoulis, T. Kibédi, At. Data Nucl. Data Tables 103–104 (2015) 50.
- [25] G.D. Dracoulis, G.J. Lane, F.G. Kondev, H. Watanabe, D. Seweryniak, S. Zhu, M.P. Carpenter, C.J. Chiara, R.V.F. Janssens, T. Lauritsen, C.J. Lister, E.A. McCutchan, I. Stefanescu, Phys. Rev. C 79 (2009) 061303.
- [26] F.W.N. de Boer, P.F.A. Goudsmit, B.J. Meijer, J.C. Kapteyn, J. Konijn, R. Kamermans, Nucl. Phys. A 263 (3) (1976) 397.
- [27] P.M. Walker, G.D. Dracoulis, A.P. Byrne, T. Kibédi, A.E. Stuchbery, Phys. Rev. C 49 (1994) 1718.
- [28] L. Wilets, M. Jean, Phys. Rev. 102 (1956) 788.
- [29] G.J. Lane, G.D. Dracoulis, F.G. Kondev, R.O. Hughes, H. Watanabe, A.P. Byrne, M.P. Carpenter, C.J. Chiara, P. Chowdhury, R.V.F. Janssens, T. Lauritsen, C.J. Lister, E.A. McCutchan, D. Seweryniak, I. Stefanescu, S. Zhu, Phys. Rev. C 82 (2010) 051304.
- [30] G.D. Dracoulis, G.J. Lane, A.P. Byrne, H. Watanabe, R.O. Hughes, F.G. Kondev, M. Carpenter, R.V.F. Janssens, T. Lauritsen, C.J. Lister, D. Seweryniak, S. Zhu, P. Chowdhury, Y. Shi, F.R. Xu, Phys. Lett. B 720 (4–5) (2013) 330.
- [31] H.L. Yadav, M. Kaushik, I.R. Jakhar, A. Ansari, Part. Nucl. Lett. 112 (2002) 66.
- [32] P.H. Regan, F.R. Xu, P.M. Walker, M. Oi, A.K. Rath, P.D. Stevenson, Phys. Rev. C 65 (2002) 037302.
- [33] A.K. Rath, P.D. Stevenson, P.H. Regan, F.R. Xu, P.M. Walker, Phys. Rev. C 68 (2003) 044315.
- [34] C.E. Vargas, V. Velázquez, S. Lerma, Eur. Phys. J. A 49 (1) (2013) 1.
- [35] J. Bartel, P. Quentin, M. Brack, C. Guet, H.-B. Håkansson, Nucl. Phys. A 386 (1) (1982) 79.
- [36] K. Yoshida, H. Watanabe, submitted for publication.
- [37] J. Terasaki, J. Engel, Phys. Rev. C 84 (2011) 014332.
- [38] V.O. Nesterenko, V.G. Kartavenko, W. Kleinig, J. Kvasil, A. Repko, R.V. Jolos, P.-G. Reinhard, Phys. Rev. C 93 (2016) 034301.